14th European Signal Processing Conference (EUSIPCO 2006), Florence, Italy, September 4-8, 2006, copyright by EURASIP

S-METHOD IN RADAR IMAGING

LJ. Stanković, T. Thayaparan**, M. Daković*, V. Popović**

* Elektrotehnički fakultet, University of Montenegro, Podgorica, Serbia and Montenegro
** Radar Applications and Space Technology, Defence Research and Development Canada, Ottawa, Canada

ABSTRACT

Commonly used technique for the SAR and ISAR signal analysis is a two-dimensional Fourier transform. Moving targets in SAR or maneuvering targets in ISAR case, induce Doppler-shift and Doppler spread in the returned signal, producing blurred or smeared images. Standard techniques for the solution of these problems are motion compensation and time-frequency analysis based techniques. Both of them are computationally intensive. Here, we will present a numerically simple S-method based approach that belongs to the time-frequency techniques. Beside the basic S-method here we will present the signal adaptive form and two-dimensional form of this method. They improve readability of the radar images what will be demonstrated on the simulated SAR and ISAR setups.

1. INTRODUCTION

Two-dimensional Fourier transform (2D FT) of the coherently processed radar echoes is conventional approach in obtaining high resolution radar images by using Synthetic Aperture Radar (SAR) or Inverse Synthetic Aperture Radar (ISAR). It will give satisfactory results (sharp images) in cases of stationary targets in the SAR applications and targets with constant and slow relative rotation in the ISAR applications. If the target is not stationary in the SAR, or performs maneuvers or observation time is high in the ISAR case, received radar signal will be frequency modulated, and 2D FT will be spread, resulting in the blurred image. In these cases motion compensation [3, 11] or time-frequency analysis based approach [3, 4, 10] is used in order to improve images readability.

This paper presents one computationally efficient technique based on the S-method [5]. Radar image is produced starting with conventionally obtained 2D FT and performing an additional simple matrix calculation. Signal dependent and two-dimensional S-method are modifications of the basic form with increased calculation complexity and better results in some specific cases [7, 8].

Basic principles of the SAR and ISAR imaging are given in Section 2. Simplified radar signal model is presented in Section 3. In Section 4 S-method and its modifications are explained and applied to the simulated examples in Section 5.

2. SAR AND ISAR IMAGING

The SAR and ISAR are methods for obtaining high resolution images of a targets. In both cases of the target imaging, high resolution in range is attained by transmitting a signal with a large bandwidth, whereas high resolution in cross-range can be achieved by utilizing the relative motion between the target and the radar to form a large synthetic aperture. Images are obtained as a result of the coherent processing of signals received from a sequence of locations. Slant range or range is the dimension along the radar line-of-sight to the target. The dimension perpendicular to the range is addressed as a cross-range.

SAR processors are typically designed to image stationary targets. In the ISAR case, the motion of the target is desirable since the information about target positions are obtained based on the changes in the viewing angle of the target with respect to the fixed radar. In these cases information about the target position in the range/cross-range domain will be contained in two-dimensional sinusoids with corresponding frequencies. Hence, range/cross-range position can be easily obtained by using 2D FT.

A moving target in the SAR induces Doppler shift and Doppler spread on the returned signal mainly in the cross-range domain. The moving target velocity component in the radar's along-track direction induces spread in the cross-range domain, while the radial velocity component is responsible for the frequency shift. Acceleration causes additional defocusing. In the ISAR case with a longer observation time intervals the target point velocity changes its direction, resulting in the corresponding frequency changes. For maneuvering targets with nonuniform equivalent rotational motion, the Doppler shift, corresponding to the cross-range of each scatterer, is time varying. The result of these motions will be frequency modulations of the returned radar signal. The 2D FT of these kind of signals will be blurred or smeared. Hence, 2D FT is not a proper tool for the radar signal observations in these cases.

3. SIGNAL MODEL

A continuous wave radar transmits signal in a form of coherent series of chirps

$$s_p(t) = \begin{cases} e^{j\pi B f_r t^2} & \text{for } 0 \le t \le T_r \\ 0 & \text{otherwise} \end{cases} \qquad (1)$$

where T_r is pulse repetition time, $f_r = 1/T_r$ is pulse repetition frequency and B is frequency bandwidth of the transmitted pulse. In one revisit the radar transmits series of M chirps

$$s(t) = e^{-j\omega_0 t} \sum_{m=0}^{M-1} s_p(t - mT_r) \tag{2}$$

where ω_0 is radar operating frequency. Total signal duration (coherent integration time or observation time) is $T_c = MT_r$.

In the literature, for example [3], the received baseband signal produced by the m-th chirp from (2) returned from the single point scatterer is described by

$$x(m,t) = \sigma e^{j\omega_0 \frac{2d}{c}} e^{-j2\pi B f_r (t - mT_r)\frac{2d}{c}}, \tag{3}$$

where σ is the reflection coefficient and d is the distance from target to radar. The two-dimensional discrete signal is obtained by sampling in time with $t - mT_r = nT_s$

$$x(n,m) = \sigma e^{j\omega_0 \frac{2d}{c}} e^{-j2\pi B f_r n T_s \frac{2d}{c}}. \tag{4}$$

Note that distance $d = d(t) = d(nT_s + mT_r)$ is time dependent when there exists target motion relative to radar. For targets with constant velocity (along radar line of sight) we have $d(t) = d_0 + v_0 t$. The first term in (3) becomes periodic with instantaneous frequency proportional to the target velocity. When target accelerates this term can be expressed as a linearly frequency modulated signal with modulation rate proportional to the target acceleration.

In the SAR setup it is assumed that the target stationary (or with slow motion) while the radar is (fast) moving (mounted on the plane or satellite). The ISAR setup assumes stationary radar (ground, or stationary vehicle mounted) and (fast) moving target. In both cases we have similar mathematical model, and we have to analyze the signals of form (4).

Signal reflected from N_s point scatterers can be expressed as a sum of individual echoes by the superposition principle.

4. S-METHOD

The S-method is time-frequency distribution highly applicable to the nonstationary multicomponent signals. It is defined in the continuous time domain [5] as

$$SM(t,\omega) = \frac{1}{2\pi} \int_{-\infty}^{\infty} P(\theta) F(t, \omega + \frac{\theta}{2}) F^*(t, \omega - \frac{\theta}{2}) d\theta \tag{5}$$

where $P(\theta)$ represents (frequency domain) window and $F(t,\omega)$ is the short-time Fourier transform of the analyzed signal $x(t)$ calculated with the lag window $w(\tau)$

$$F(t,\omega) = \int_{-\infty}^{\infty} w(\tau) x(t+\tau) e^{-j\omega\tau} d\tau. \tag{6}$$

It is proven that for special cases of the window $P(\theta) = \delta(\theta)$ the S-method is equal to the spectrogram $SPEC(t,\omega) = |F(t,\omega)|^2$ of the analyzed signal and for $P(\theta) = 1$ the S-method is equal to the pseudo Wigner distribution of the analyzed signal

$$WD(t,\omega) = \int_{-\infty}^{\infty} w(\frac{\tau}{2}) w^*(\frac{\tau}{2}) x(t + \frac{\tau}{2}) x^*(t - \frac{\tau}{2}) e^{-j\omega\tau} d\tau \tag{7}$$

These two time-frequency distributions have very different properties. While spectrogram is almost cross-terms free distribution it have very low concentration in the case of nonstationary signals. On the other hand Wigner distribution produces highly concentrated auto-terms, but in the case of multicomponent signals there exist strong cross-terms. By an adequately chosen window $P(\theta)$ we can combine good properties of both distributions avoiding undesired effects.

4.1 Discrete S-method

Discrete forms of the S-method reads

$$SM(n,k) = \sum_{i=-L}^{L} P(i) F(n, k+i) F^*(n, k-i) \tag{8}$$

where we assume that window $P(i)$ is finite of the length $2L+1$ samples. Discrete form of the short-time Fourier transform is

$$F(n,k) = \sum_{m=-N/2}^{N/2-1} w(m) x(n+m) e^{-j\frac{2\pi}{N}mk}. \tag{9}$$

If we assume that window $P(i)$ is rectangular, then we can calculate the S-method recursively as

$$SM_L(n,k) = SM_{L-1}(n,k) + 2\Re[F(n,k+L)F^*(n,k-L)]$$

for $L = 1, 2, \ldots$ where $\Re[\cdot]$ stands for real part, starting with

$$SM_0(n,k) = |F(n,k)|^2.$$

4.2 Adaptive S-method

Signal-dependent or adaptive S-method is presented in [7]. The main idea is to limit summation in (8) to the auto-terms only. In this way we can avoid situation where $F(n,k+i)$ belongs to one component and $F^*(n,k-i)$ belongs to another component. One approach is to stop summation in (8) when zero value is detected, but the true zero values in the Fourier transform are very sensitive to noise and even to numerical errors. Another approach is to use the reference level R_L. Summation stops when the value of either $|F(n,k+i)|$ or $|F(n,k-i)|$ falls below R_L. A good choice of R_L is few percent of the maximal value of $|F(n,k)|$.

4.3 Two-dimensional S-method

The S-method can be applied in both analyzed radar image dimensions. Then we can use two-dimensional

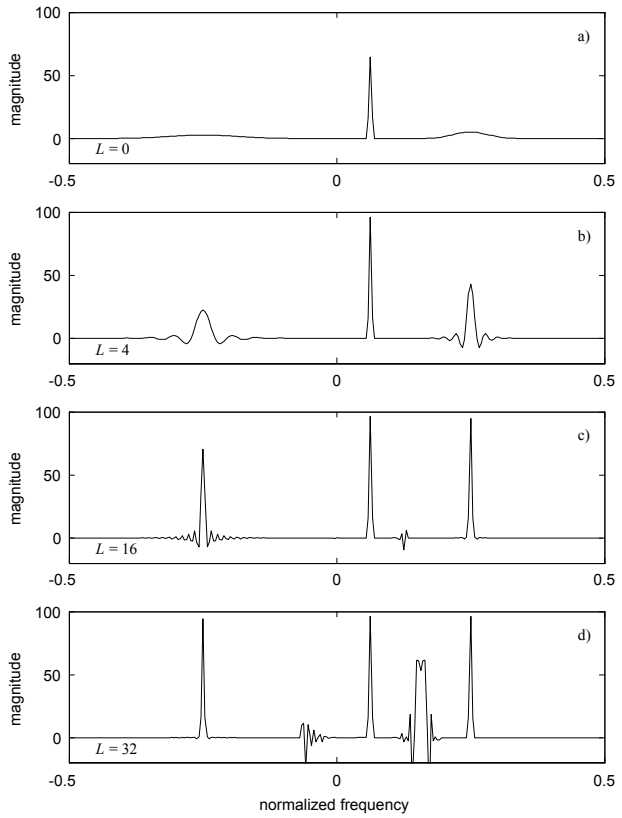

Figure 1: S-method of a three-component signal: a) $L = 0$ - spectrogram, b) $L = 4$, c) $L = 16$ and d) $L = 32$

S-method form [8]. Basic formula is

$$SM_{2D}(n_1, k_1, n_2, k_2) = \sum_{l_1=-L_1}^{L_1} \sum_{l_2=-L_2}^{L_2} P(l_1, l_2) \times$$

$$\times F_{2D}(n_1, k_1 + l_1, n_2, k_2 + l_2) F^*_{2D}(n_1, k_1 - l_1, n_2, k_2 - l_2)$$

where F_{2D} represents two-dimensional short-time Fourier transform of the analyzed signal $x(n_1, n_2)$

$$F_{2D}(n_1, k_1, n_2, k_2) =$$

$$\sum_{i_1=-\frac{N_1}{2}}^{\frac{N_1}{2}-1} \sum_{i_2=-\frac{N_2}{2}}^{\frac{N_2}{2}-1} x(n_1 + i_1, n_2 + i_2) w(i_1, i_2) e^{-j2\pi(\frac{i_1 k_1}{N_1} + \frac{i_2 k_2}{N_2})}$$

where N_1 and N_2 stands for the number of samples along n_1 and n_2 axes respectively and $w(i_1, i_2)$ is a two-dimensional lag window.

Although this approach seams to be natural in the radar imaging, in most applications radar images are enough sharp in the range direction, so the one dimensional S-method applied to the cross-range direction gives satisfactory results with lower calculation complexity.

4.4 S-method example

The S-method application will be demonstrated on the simulated example. We consider three component signal, where the signal components can be associated with returned radar signals from three targets (points). The second target has constant velocity, while the first and the third target accelerates. This signal can be modelled as

$$x(n) = x_1(n) + x_2(n) + x_3(n)$$

with

$$\begin{aligned} x_1(n) &= A(n) e^{-j\frac{0.4}{256}\pi n^2} e^{-j\frac{\pi}{2}n} \\ x_2(n) &= A(n) e^{j\frac{\pi}{8}n} \\ x_3(n) &= A(n) e^{j\frac{0.2}{256}\pi n^2} e^{j\frac{\pi}{2}n} \end{aligned}$$

where the amplitude $A(n)$ is slow-varying, defined as $A(n) = \frac{1}{2} + \frac{1}{2}\cos\frac{\pi}{256}n$. The signal is defined for $-128 \leq n \leq 127$. Note that the first and the third signal component are linear frequency modulated (LFM) with discrete instantaneous frequencies $\omega_1(n) = -\frac{0.4}{128}\pi n - \frac{\pi}{2}$ and $\omega_3(n) = \frac{0.2}{128}\pi n + \frac{\pi}{2}$, while the second component has constant frequency $\omega_2 = \frac{\pi}{8}$. At the considered time instant ($n = 0$) we have $\omega_1(0) = -\frac{\pi}{2}$, $\omega_2(n) = \frac{\pi}{8}$ and $\omega_3(0) = \frac{\pi}{2}$.

Figure 1 presents S-method of the analyzed signal calculated at the time instant $n = 0$ for $L = 0, 4, 16$ and 32 respectively. Due to the frequency modulation the second and the third component in the spectrogram (S-method with $L = 0$, Fig.1.a) are spread and not visible as compared to the highly concentrated constant-frequency component. For $L = 4$ (Fig.1.b) we can see improvement in the concentration of the LFM components. For higher values of L ($L = 16$ and $L = 32$, Fig.1.c and d) component concentration increases, but undesired cross-terms appear between components.

The adaptive S-method is applied to the same signal and results are presented in Fig.2 (upper subplot). The values of L for each frequency sample k used in (8) are presented in the lower subplot. As we can see high values of L are used in order to obtain high concentration of the LFM components and very low values (even $L = 0$) are used where concentration improvement is unnecessary. The reference level in this example is set to 3% of the maximal absolute value of the Fourier transform.

5. RADAR IMAGING EXAMPLES

5.1 SAR example

Let us consider airborne SAR with 10 GHz operating frequency, 250 MHz bandwidth, 200 Hz pulse repetition frequency, 128 pulses in one revisit. Plane is moving along x-axis with velocity $V_{plane} = 100\frac{\text{m}}{\text{s}}$. Plane altitude is $h_{plane} = 2000$ m. Incidence angle at the targets is 45°. Here we will consider seven targets setup where each target can be modeled as a single point scatterer. Five targets are stationary and remaining two are moving along x-axis with constant velocities. The target coordinates and velocities are presented in Table 1.

Conventional SAR image is obtained as 2D FT of the coherently processed and range-compensated returned signals and is shown in the Fig.3 (upper left subplot).

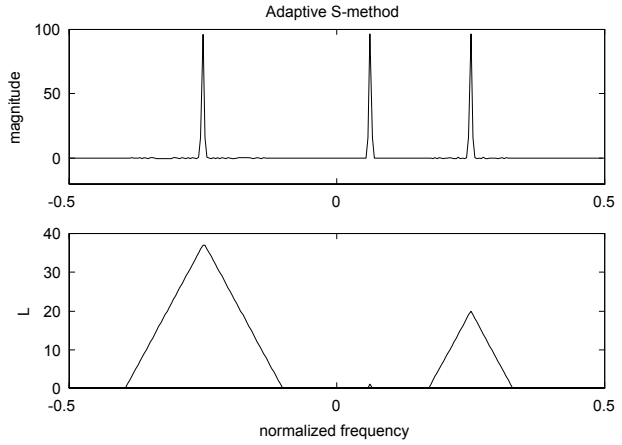

Figure 2: Adaptive S-method of a three-component signal (upper subplot). Values of L for each frequency sample (lower subplot)

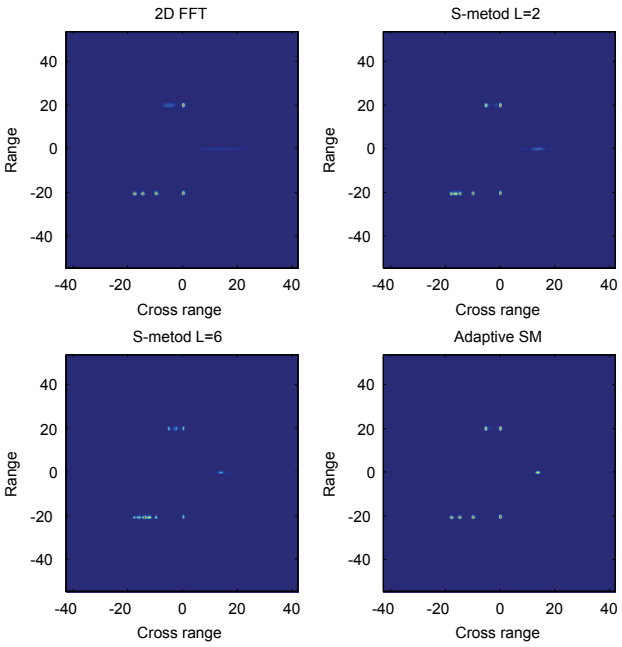

Figure 3: Simulated SAR images obtained by 2D FT (upper left), S-method with $L = 2$ (upper right), $L = 6$ (lower left) and adaptive S-method (lower right)

Scatterer No	1	2	3	4	5	6	7
x [m]	0	-10	-15	-18	0	20	-5
y [m]	-20	-20	-20	-20	20	0	20
V_x [$\frac{\text{m}}{\text{s}}$]	0	0	0	0	0	30	-5

Table 1: Positions and velocities of targets (SAR exapmple)

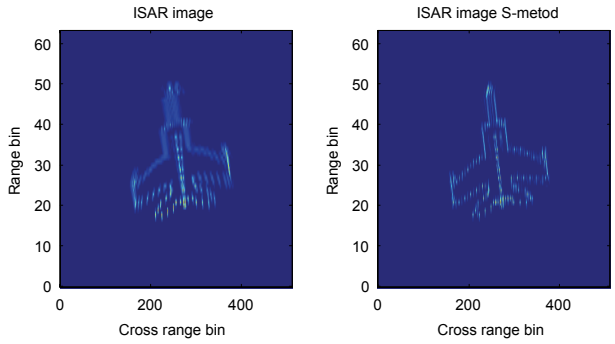

Figure 4: ISAR image obtained by 2D FT (left) and S-method with $L = 5$ (right) for simulated MIG25 dataset.

As one can see stationary targets are clearly presented, while two moving scatterers are blurred. The fast moving scatterer No.6 is even visually undetectable. By applying the S-method based postprocessing of the obtained 2D FT with $L = 2$ (Fig.3 upper right subplot) moving targets becomes more concentrated, but there is undesired cross-term between targets No.3 and No.4. Higher value of L (Fig.3 lower left subplot) improves concentration of the moving targets, but new cross-terms also appear between targets No.5 and No.7 and targets No.2 and No.3. Adaptive S-method presented in Fig.3 (lower right subplot) gives moving targets concentrated as stationary targets, and without undesired cross-terms.

Note that the moving targets are dislocated in the cross-range direction due to the non-negligible projection of the scatterers velocity to the radar line of sight in each dwell.

5.2 ISAR examples

We tested our approach on the simulated MIG25 dataset described in [3]. The S-method with $L = 5$ applied to the cross-range dimension significantly improves image readability as it is presented in the Fig.4 (right) compared to the conventional 2D FT (Fig.4, left).

In the sequel we considered ISAR working at 10 GHz with 2 GHz bandwidth, pulse repetition frequency of 200 Hz, 256 pulses in one revisit and 256 samples within each pulse. The target is simulated as eleven point scatterers in (x, y) plane with altitude $h = 100$ m. The scatterers coordinates are presented in the Table 2. Target is moving with constant velocity $V_T = 100\frac{\text{m}}{\text{s}}$ along x-axis. Radar is located at the ground coordinates $(x_R, y_R) = (-50\,\text{m}, 200\,\text{m})$. Returned signal (after coherent processing and range compensation) is processed and results are presented in Fig.5. Upper left subplot is image obtained in classical manner as a 2D FT of the returned signal. As one can see image is unfocused. Image obtained by the two-dimensional S-method with $L_1 = L_2 = 5$ (upper right subplot) is very sharp with good geometry. One-dimensional S-method applied to

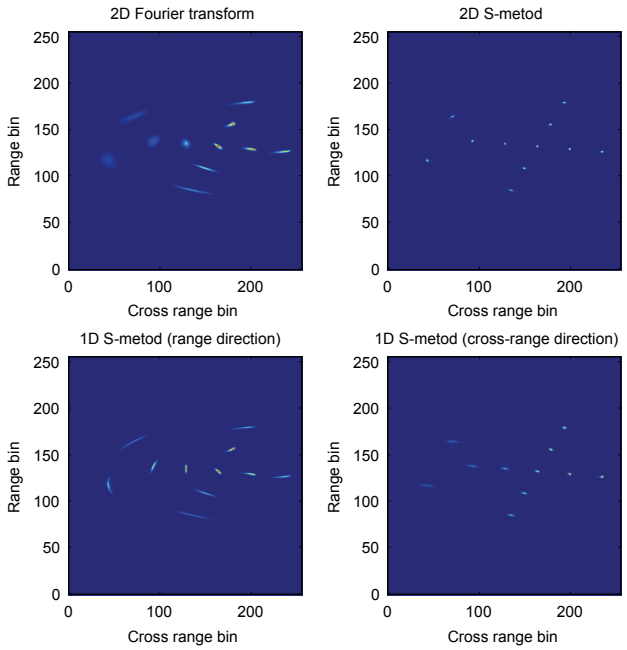

Figure 5: Simulated ISAR setup: ISAR image obtained by: 2D Fourier transform (upper left), 2D S-method (upper right), and 1D S-method applied along range (lower left) and cross-range (lower right) direction.

No	1	2	3	4	5	6	7	8	9	10	11
x	-2	-2	-1	0	1	1	1	1	1	2	3
y	-2	2	0	0	0	2	4	-2	-4	0	0

Table 2: Positions of the scatterers (ISAR example)

the cross-range direction (lower right subplot) also give satisfactory results, slightly worse than 2D S-method. Lower left subplot in Fig.5 demonstrates that application of the S-method along range dimension only, does not produce significant image improvement. Note that radar and target parameters not correspond to the real radar setups because we wanted to emphasize situation where 2D S-method significantly improve image sharpness.

6. CONCLUSION

In some cases the 2D FT is not a good tool for obtaining SAR or ISAR images. A numerically simple S-method based approach is presented as a tool for improving images readability in such cases. Furthermore, two modifications of the basic form, adaptive and two-dimensional S-method are presented. Since the S-method is obtained by making slight correction of the results already obtained by the Fourier based algorithm, it is computationally efficient comparing to the time-frequency based and motion compensation methods available in the literature. By using the SAR and ISAR setups it is proved that these techniques can improve readability of the SAR and ISAR images.

REFERENCES

[1] B. Boashash, Ed., *Time-frequency signal analysis and processing*, Elsevier, 2003

[2] L. Cohen, *Time-frequency analysis,* Prentice-Hall Inc., New York, USA, 1995

[3] V.C. Chen, *Time-Frequency Transforms for Radar Imaging and Signal Analysis*, Artech House, 2002

[4] H. Ling, Y. Wang, V. C. Chen, "ISAR image formation and feature extraction using adaptive joint time-frequency processing", SPIE Proc. on Wavelet Applications, Vol.3708, Apr.1997, pp.424-432.

[5] LJ. Stanković, "A method for time-frequency analysis", *IEEE Trans. on Signal Processing*, Vol. 42, No.1, Jan. 1994, pp. 225-229.

[6] LJ. Stanković, T. Thayaparan, M. Daković: "Improvement of the fast moving targets presentation in ISAR by using the S-method", *13-th European Signal Processing Conference*, September 4-8, 2005, Antalya, Turkey.

[7] S.Stanković, LJ.Stanković, "An architecture for the realization of a system for time-frequency signal analysis", *IEEE Trans. on Circuits and Systems*, Part II, No.7, July 1997, pp.600-604.

[8] S. Stanković, I. Djurović, V. Vuković, "System architecture for Space-Frequency Image Analysis", *Electronic Letters*, Vol.34, No.23, Nov.1998, pp. 224-225.

[9] V. Popović, M. Daković, T. Thayaparan, LJ. Stanković: "SAR Images Improvements by Using the S-Method", *31-st International Conference on Acoustics, Speech, and Signal Processing (ICASSP),* May 14-19, 2006, Toulouse, France.

[10] Y. Wang, H. Ling, V. C. Chen: "ISAR Motion Compensation Via Adaptive Joint Time-Frequency Technique", *IEEE Trans. Aerospace and Electronic Systems*, Vol.34, No.4, Apr.1990, pp.670-677.

[11] S. Werness, W. Carrara, L. Joyce: "Moving target imaging algorithm for SAR data", *IEEE Trans. Aerospace and Electronic Systems*, Vol.26, No.1, Jan.1990, pp.57-67.